

Dissecting Sites Important for Complement Regulatory Activity in Membrane Cofactor Protein (MCP; CD46)*

Received for publication, May 30, 2000, and in revised form, August 22, 2000
Published, JBC Papers in Press, August 25, 2000, DOI 10.1074/jbc.M004650200

M. Kathryn Liszewski[‡], Marilyn Leung[‡], Wenying Cui[‡], V. Bala Subramanian[‡], John Parkinson[§], Paul N. Barlow[§], Marianne Manchester[¶], and John P. Atkinson[‡]||

From the [‡]Division of Rheumatology, Department of Medicine, Washington University School of Medicine, St. Louis, Missouri 63110, the [¶]Division of Virology, Department of Neuropharmacology, Scripps Research Institute, La Jolla, California 92037, and the [§]Edinburgh Centre for Protein Technology, Joseph Black Chemistry Building, West Mains Road, Edinburgh EH9 3JJ, Scotland

Membrane cofactor protein (MCP; CD46), a widely distributed regulator of complement activation, is a cofactor for the factor I-mediated degradation of C3b and C4b deposited on host cells. MCP possesses four extracellular, contiguous complement control protein modules (CCPs) important for this inhibitory activity. The goal of the present study was to delineate functional sites within these modules. We employed multiple approaches including mutagenesis, epitope mapping, and comparisons to primate MCP to make the following observations. First, functional sites were located to each of the four CCPs. Second, some residues were important for both C3b and C4b interactions while others were specific for one or the other. Third, while a reduction in ligand binding was invariably accompanied by a parallel reduction in cofactor activity (CA), other mutants lost or had reduced CA but retained ligand binding. Fourth, two C4b-regulatory domains overlapped measles virus interactive regions, indicating that the hemagglutinin docks to a site important for complement inhibition. Fifth, several MCP regulatory areas corresponded to functionally critical, homologous positions in other CCP-bearing C3b/C4b-binding proteins. Based on these data and the recently derived crystal structure of repeats one and two, computer modeling was employed to predict MCP structure and examine active sites.

Membrane cofactor protein (MCP¹; CD46) is a widely expressed type 1 transmembrane glycoprotein that regulates complement activation (reviewed in Ref. 1). It serves as a cofactor for the plasma serine protease factor I to cleave C3b

and C4b that deposit on host tissue. MCP belongs to a family of structurally, functionally, and genetically related receptor and inhibitory proteins called the regulators of complement activation (RCA) (reviewed in Ref. 1). Other members are complement receptors one (CR1; CD35) and two (CR2; CD21), decay accelerating factor (DAF; CD55), and two plasma proteins, factor H and C4b-binding protein (C4BP). The amino-terminal regions of these proteins consist of variable numbers (from 4 to 30) of tandemly-linked, independently folding, cysteine-rich modules of approximately 60 amino acids termed complement control protein (CCP) repeats. The elliptical CCP modules possess hydrophobic cores with characteristic β -sheet-rich secondary structures and interact with C3b and C4b.

Perhaps owing to both its abundant expression and regulatory role, MCP is the target of several pathogens. It is a receptor for measles virus (MV) (2–4), group A *Streptococcus pyogenes* (5), pathogenic *Neisseria* species (6), and human herpesvirus 6 (7). Additionally, other pathogens (e.g. pox viruses) synthesize complement inhibitory proteins (virulence factors) that functionally and, in some cases, structurally resemble MCP or other complement inhibitors (8). Additional roles for MCP include its association with β_1 integrins and tetraspans (9), putative involvement in reproduction (10–15), and use as a therapeutic agent both as a recombinant soluble form (16) and if expressed in transgenic animals for organ xenotransplantation (reviewed in Refs. 17 and 18).

Most cells express MCP as a family of four alternatively spliced isoforms that share an identical amino-terminal portion consisting of four CCP modules (19, 20). Next is the variably spliced region for O-glycosylation called the STP domain, which is enriched in serines, threonines, and prolines. This is followed by a 12-amino acid segment of undefined function, a transmembrane domain, cytoplasmic anchor, and one of two alternatively spliced cytoplasmic tails.

Sites for C3b and C4b interactions have been mapped by CCP deletions primarily to modules 2, 3, and 4 (21, 22). Additionally, the MV binding site has been localized to CCPs 1 and 2 (22–26). The aim of the present study was to identify areas in the CCP domains that are important for C3b and C4b binding and cofactor activity (CA). We report on functional insights provided by (a) an analysis of 55 mutants, (b) the binding of ligands to MCP peptides, (c) comparisons to the functional profile of primate MCPs, and (d) mapping the epitope of a function-blocking mAb. Based on these results and a recently determined crystal structure of CCPs 1 and 2 (27), we developed a structural model and localized putative active sites on the CCPs of MCP.

* This work was supported by National Institutes of Health Grant R01 AI37618. The costs of publication of this article were defrayed in part by the payment of page charges. This article must therefore be hereby marked "advertisement" in accordance with 18 U.S.C. Section 1734 solely to indicate this fact.

|| To whom correspondence should be addressed: Div. of Rheumatology, Washington University School of Medicine, 660 S. Euclid Ave., Box 8045, St. Louis, MO 63110. Tel.: 314-362-8391; Fax: 314-362-1366; E-mail: jatkinso@im.wustl.edu.

¹ The abbreviations used are: MCP, membrane cofactor protein; CCP, complement control protein; RCA, regulators of complement activation; CR, complement receptor; C4BP, C4b-binding protein; DAF, decay accelerating factor; MV, measles virus; CA, cofactor activity; CHO, Chinese hamster ovary; GB24 and TRA-2-10, anti-MCP monoclonal antibodies; TMB, 3,3',5,5'-tetramethylbenzidine; ELISA, enzyme-linked immunosorbent assay; TBS, Tris-buffered saline; mAb, monoclonal antibody; PAGE, polyacrylamide gel electrophoresis; BSA, bovine serum albumin.

TABLE I
Summary of mutants

Mutant	CCP	Amino acid sequence of wild-type and mutant proteins																Related tables ^a
		D	R	N	H	T	W	L	P	V	S	D	D	A	C ₄	Y		
47–61 ^b	1	D	R	N	H	T	W	L	P	V	S	D	D	A	C ₄	Y	II	
1s4 ^c	1	L	G	M	Q	—	W	S	D	I	E	E	F	—	C ₄	N	II	
94–103	2	N	E	G	Y	Y	L	I	G	E	E	—	—	—	—	—	II	
N94A	2	A	—	—	—	—	—	—	—	—	—	—	—	—	—	—	II	
E95A	2	—	A	—	—	—	—	—	—	—	—	—	—	—	—	—	II	
G96A	2	—	—	A	—	—	—	—	—	—	—	—	—	—	—	—	II	
Y97A	2	—	—	—	A	—	—	—	—	—	—	—	—	—	—	—	II	
Y98A	2	—	—	—	—	A	—	—	—	—	—	—	—	—	—	—	II	
L99A	2	—	—	—	—	—	A	—	—	—	—	—	—	—	—	—	II	
I100A	2	—	—	—	—	—	—	A	—	—	—	—	—	—	—	—	II	
E102A	2	—	—	—	—	—	—	—	—	A	—	—	—	—	—	—	II	
E103A	2	—	—	—	—	—	—	—	—	—	A	—	—	—	—	—	II	
102–112	2	E	E	I	L	Y	C ₃	E	L	K	G	S	—	—	—	—	IV	
Primate A ^d	2	K	D	—	—	—	—	—	—	—	D	T	—	—	—	—	IV	
118–122	2	G	K	P	P	I	—	—	—	—	—	—	—	—	—	—	II/V	
G118A	2	A	—	—	—	—	—	—	—	—	—	—	—	—	—	—	II/V	
K119A	2	—	A	—	—	—	—	—	—	—	—	—	—	—	—	—	II/V	
P120A	2	—	—	A	—	—	—	—	—	—	—	—	—	—	—	—	II/V	
P121A	2	—	—	—	A	—	—	—	—	—	—	—	—	—	—	—	II/V	
I122A	2	—	—	—	—	A	—	—	—	—	—	—	—	—	—	—	II/V	
122–126	2	I	C ₄	E	K	V	—	—	—	—	—	—	—	—	—	—	IV	
Primate B	2	L	—	—	—	I	—	—	—	—	—	—	—	—	—	—	IV	
127–134	3	L	C ₁	T	P	P	P	K	I	—	—	—	—	—	—	—	V/VI	
127–134 ^c	3	D	C ₁	G	L	P	P	D	V	—	—	—	—	—	—	—	V/VI	
T129A/P130A	3	—	—	A	A	—	—	—	—	—	—	—	—	—	—	—	V/VI	
I134A	3	—	—	—	—	—	—	—	A	—	—	—	—	—	—	—	V/VI	
151–165	3	D	A	V	T	Y	S	C ₂	D	P	A	P	G	P	D	P	III/V	
151–158 ^c	3	T	V	I	T	Y	K	C ₂	E	—	—	—	—	—	—	—	III/V	
D158A/P159A	3	—	—	—	—	—	—	—	A	A	—	—	—	—	—	—	III/V	
P161A	3	—	—	—	—	—	—	—	—	—	A	—	—	—	—	—	III/V	
G162A/P163A	3	—	—	—	—	—	—	—	—	—	—	—	A	A	—	—	III/V	
D164A/P165A	3	—	—	—	—	—	—	—	—	—	—	—	—	—	A	A	III/V	
174–184	3	T	I	Y	C ₃	G	D	N	S	V	W	S	—	—	—	—	IV	
Primate C	3	M	—	—	—	—	N	—	—	T	—	H	—	—	—	—	IV	
183–191	3	S	R	A	A	P	E	C ₄	K	V	—	—	—	—	—	—	V/VI	
183–190 ^c	3	S	D	I	E	E	F	C ₄	N	—	—	—	—	—	—	—	V/VI	
S183T	3	T	—	—	—	—	—	—	—	—	—	—	—	—	—	—	V/VI	
R184K	3	—	K	—	—	—	—	—	—	—	—	—	—	—	—	—	V/VI	
A185I	3	—	—	I	—	—	—	—	—	—	—	—	—	—	—	—	V/VI	
E188F	3	—	—	—	—	—	F	—	—	—	—	—	—	—	—	—	V/VI	
V191D	3	—	—	—	—	—	—	—	—	D	—	—	—	—	—	—	V/VI	
193–197	4	K	C ₁	R	F	P	—	—	—	—	—	—	—	—	—	—	V/VI	
193–197 ^c	4	D	C ₁	G	L	P	—	—	—	—	—	—	—	—	—	—	V/VI	
K193A	4	A	—	—	—	—	—	—	—	—	—	—	—	—	—	—	V/VI	
R195A	4	—	—	A	—	—	—	—	—	—	—	—	—	—	—	—	V/VI	
F196A	4	—	—	—	A	—	—	—	—	—	—	—	—	—	—	—	V/VI	
P197A	4	—	—	—	—	A	—	—	—	—	—	—	—	—	—	—	V/VI	
205–212	4	I	S	G	F	G	K	K	F	—	—	—	—	—	—	—	V/VI	
205–212 ^c	4	S	F	P	E	D	T	V	I	—	—	—	—	—	—	—	V/VI	
I205A	4	A	—	—	—	—	—	—	—	—	—	—	—	—	—	—	V/VI	
S206A	4	—	A	—	—	—	—	—	—	—	—	—	—	—	—	—	V/VI	
G207A	4	—	—	A	—	—	—	—	—	—	—	—	—	—	—	—	V/VI	
F208A	4	—	—	—	A	—	—	—	—	—	—	—	—	—	—	—	V/VI	
G209A	4	—	—	—	—	A	—	—	—	—	—	—	—	—	—	—	V/VI	
K210A	4	—	—	—	—	—	A	—	—	—	—	—	—	—	—	—	V/VI	
K211A	4	—	—	—	—	—	—	A	—	—	—	—	—	—	—	—	V/VI	
F212A	4	—	—	—	—	—	—	—	A	—	—	—	—	—	—	—	V/VI	
226–233	4	F	Y	L	D	G	S	D	T	—	—	—	—	—	—	—	IV	
Primate D	4	Y	—	—	N	—	—	—	K	—	—	—	—	—	—	—	IV	
243–250	4	D	P	P	V	P	K	C ₄	L	—	—	—	—	—	—	—	V/VI	
243–250 ^c	4	S	D	I	E	E	F	C ₄	N	—	—	—	—	—	—	—	V/VI	
D243A	4	A	—	—	—	—	—	—	—	—	—	—	—	—	—	—	V/VI	
P244A	4	—	A	—	—	—	—	—	—	—	—	—	—	—	—	—	V/VI	
P245A	4	—	—	A	—	—	—	—	—	—	—	—	—	—	—	—	V/VI	
V246A	4	—	—	—	A	—	—	—	—	—	—	—	—	—	—	—	V/VI	

^a Functional analyses are presented in the table(s) as noted.

^b Hyphenated numbers indicate wild-type residues. Mutants G101A, K133A, P187A, and K190A were not expressed. Mutations were not prepared for the cysteine residue of a series, *e.g.* Cys¹²⁸, Cys¹⁵⁷, Cys¹⁸⁹, Cys¹⁹⁴, and Cys²⁴⁹. Subscripts indicate which of the four cysteines in a CCP it represents.

^c Substituted sequence from homologous region of CCP 1 of human DAF.

^d Primates A–D represent substitutions of baboon/rhesus residues into the human sequence.

EXPERIMENTAL PROCEDURES

Mutagenesis and Expression—Substitutions were produced utilizing the QuikChange[™] site-directed mutagenesis kit (Stratagene Cloning Systems, La Jolla, CA) per the manufacturer's directions. The template was MCP isoform BC1 (GenBank[™] accession no. X59405) cloned into the *EcoRI* site of plasmid pSG5 (Stratagene). All cDNA clones were sequenced in their entirety. Transient transfections were either performed with Lipofectin (Life Technologies, Inc.) or Fugene-6 (Roche Molecular Biochemicals) into Chinese hamster ovary K1 (CHO) cells per manufacturer's directions. CHO cells were maintained in Ham's F-12 medium supplemented with 10% fetal calf serum and penicillin/streptomycin.

Quantification of MCP—MCP-expressing cells were characterized by Western blotting and ELISA as described previously (28). Nucleated cells were lysed in 1% Nonidet P-40, 0.05% SDS, and 2 mM phenylmethylsulfonyl fluoride in TBS (10 mM Tris, pH 7.2, 150 mM sodium chloride) and supernatants collected following centrifugation at $12,000 \times g$. Erythrocytes were isolated from primate blood (obtained from Yerkes Primate Research Center, Atlanta, GA) and lysed as described previously (29). MCP was quantified by ELISA (28). Briefly, an MCP mAb

(TRA-2-10) was coated on microtiter wells (5 $\mu\text{g/ml}$) in TBS overnight at 4 °C followed by blocking with 1% BSA and 0.1% Tween 20. Cell lysates were prepared in 10 mM Tris, 150 mM sodium chloride, 0.05% Tween 20, 4% BSA, and 0.25% Nonidet P-40. These samples and standards were incubated for 1 h at 37 °C and then washed with TBS containing 0.05% Tween 20. Next, rabbit anti-MCP antiserum (1:7000) (provided by CytoMed, Inc. Cambridge, MA) was applied for 1 h at 37 °C. After washing, horseradish peroxidase-coupled donkey anti-rabbit IgG (Jackson ImmunoResearch Laboratories, West Grove, PA) was added and incubated for 1 h at 37 °C. After washing, TMB substrate (Pierce) was added and absorbance (630 nm) assessed in an ELISA reader. Mutants were also characterized by Western blotting utilizing rabbit anti-MCP polyclonal antibody (28).

Functional Assessment—Ligand binding and cofactor assays have been described (28). An ELISA format was employed for ligand binding. Briefly, C3b or C4b (Advanced Research Technologies, San Diego, CA) was coated on wells at 5 $\mu\text{g/ml}$ in TBS overnight at 4 °C and then blocked for 1 h at 37 °C (1% BSA and 0.1% Tween 20 in TBS). Dilutions of lysates were prepared in low salt ELISA buffer (10 mM Tris, 25 mM sodium chloride, 0.05% Tween 20, 4% BSA, and 0.25% Nonidet-P40) and incubated for 2 h at 37 °C. A rabbit anti-MCP antiserum (1:2500) in low salt buffer was then added for 1 h at 37 °C. Following washing, a peroxidase-coupled donkey anti-rabbit IgG was added and optical density of the TMB substrate determined. Binding assays were performed on serially diluted samples (in the linear range of $1\text{--}10 \times 10^3$ MCP/ml) on three separate occasions. The upper value was utilized to compare results and the standard error of the mean was <7%.

For the cofactor assays, biotinylated ligands were employed (28) with a low salt cofactor buffer (10 mM Tris, pH 7.2, 25 mM NaCl, 1% Nonidet P-40, 2 mM phenylmethylsulfonyl fluoride), factor I (100 ng), and cell lysates (2.5×10^8 MCP for the C3b cofactor assay and 5×10^8 for the C4b cofactor assay). Cleavage fragments were analyzed utilizing 10% reducing SDS-PAGE followed by transfer and Western blotting. Detection was with ExtrAvidin[®] peroxidase conjugate (Sigma). A laser densitometer and GELscan software (Amersham Pharmacia Biotech) were employed to monitor the generation of the C4d fragment (adjusted relative to the input as measured by the γ -chain fragment of C4b). For the C3b cofactor assay, the $\alpha 1$ fragment was evaluated relative to the β -chain. Activity was designated as follows: + + + +, 90–120% of wild type; + + +, 70–89%; + +, 40–69%; +, 10–39%; –, <10%. Assays were performed in duplicate on two to four separate occasions and the means obtained. The standard error of the mean was <10%.

Peptide ELISA—The overlapping MCP-derived peptides utilized in this study have been described (24). For the ELISA, peptides were coated on microtiter wells (Nunc MaxiSorp modules, Fisher Scientific, St. Louis, MO) at 10 $\mu\text{g/ml}$ in TBS overnight at 4 °C and blocked with 1% BSA, 0.1% Tween 20 in TBS. C4b (or buffer alone) was added at a concentration of 30 ng/ml in low salt buffer (4% BSA, 0.25% Nonidet P-40 in 10 mM Tris, pH 7.2, and 25 mM sodium chloride) and incubated for 2 h at 37 °C. Wells were washed in low salt buffer (10 mM Tris, pH 7.2, 25 mM sodium chloride, 0.05% Tween 20), followed by incubation with 1:7000 dilution of goat anti-human C4b (Advanced Research Technologies) for 1 h at 37 °C. After washing in low salt ELISA buffer, peroxidase conjugated anti-globulin reagent was added for 1 h at 37 °C, wells were washed and then the TMB substrate (see above) was added.

TABLE II
Functional effects of amino acid substitutions in CCP 1 and 2

Mutant	C3b		C4b	
	Binding ^a	Cofactor ^b	Binding	Cofactor
	%		%	
RCHO ^c	1	—	2	—
MCP ^d	100	++++	100	++++
47–61 ^e	94	++++	75	++
N94A	93	++++	62	+
E95A	110	++++	67	+
G96A	107	+++	33	++
Y97A	110	+++	84	+
Y98A	103	++++	107	+
L99A	111	++	91	+
I100A	106	++++	100	+++
E102A ^f	63	++	67	+
E103A	106	++++	102	++
G118A	100	++++	100	+++
K119A	93	++++	113	+++
P120A	115	+++	97	++
P121A	120	+++	119	+
I122A	107	+++	111	+

^a Wild-type MCP binding was set at 100%. Background for cofactor activity consisted of standard conditions without lysate.

^b Cofactor activity was graded as follows: + + + +, 90–120% of wild type; + + +, 70–89%; + +, 40–69%; +, 10–39%; –, <10%.

^c RCHO is the negative control (*i.e.* a CHO cell with the MCP cDNA cloned in reverse orientation).

^d MCP is the wild-type control.

^e MCP residues 47–61 were substituted for homologous residues of DAF CCP 1 (see Table I).

^f Mutant G101A was not expressed.

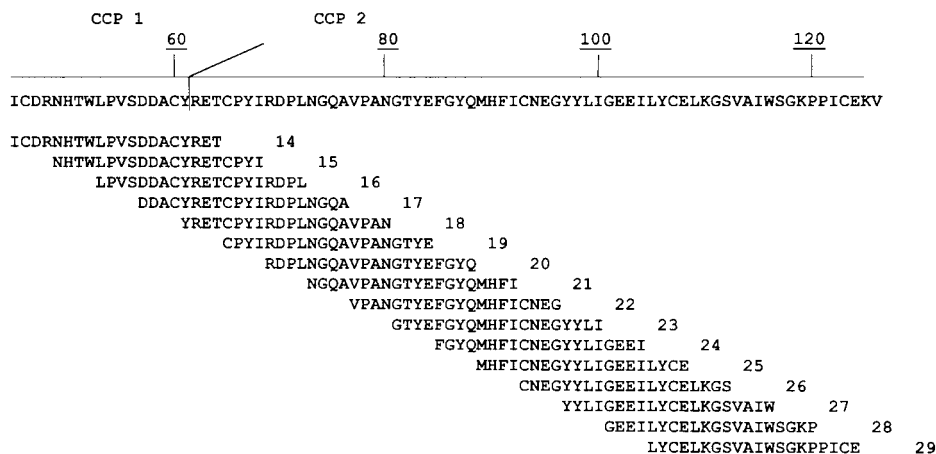


FIG. 1. Overlapping peptides from the carboxyl terminus of CCP 1 to the end of CCP 2 used to assess ligand binding. Residues are numbered according to Ref. 24.

Absorbance was measured at 630 nm. The peptides were shown to be coated on wells to a similar extent by incubating rabbit anti-MCP antiserum (1:7000) on the peptide wells followed by detection with anti-globulin and substrate as indicated above.

Epitope Mapping—These experiments were conducted as described above under “Quantification of MCP” except that TRA-2–10 (non-function blocking mAb that binds an epitope in CCP 1) (23, 30) or GB24 (function-blocking mAb that binds to an epitope requiring CCPs 3 and 4) (21, 31) were coated on the microtiter wells.

Computer Modeling—Three dimensional co-ordinates of the crystal structure of the first two modules of MCP (CCP 1 and 2) were obtained from the Brookhaven data base (27). Three-dimensional molecular models of the two C-terminal modules were constructed within the program MODELLER (32). Five models were generated per module, and in each case the model with the smallest root mean square deviations from the average was used in the subsequent interpretation of mutagenesis data and modeling exercises.

The relative orientations of CCP 2 to CCP 3 and of CCP 3 to CCP 4 were modeled using a hybrid Monte Carlo molecular dynamics algorithm previously shown to predict the relative orientations for a number of CCP module pairs.² In brief, each of the two pairs of modules of MCP were linked using the Builder module of Insight II (MSI, San Diego, CA). Further manipulations of the structures of module pairs were performed using XPLOR (33) with the charmm22 forcefield (34). Only residues within 18 Å of the linker between modules were used for the prediction algorithm. This involved the random selection of one of the ϕ/ψ angles of the two amino acids linking the module pair, and rotating it by a random amount. This was followed by a brief period of energy minimization (to allow the structure to resolve any bad contacts that may have arisen during the previous step). The resulting conformation of the two modules was then accepted with a probability (P) based on the relative change in energy with respect to the previously accepted conformation using the standard Metropolis Monte Carlo equation: $P = \min(1, e^{-\Delta E/kT})$, where ΔE = difference in energy between the old and the new conformation, k = the Boltzman constant, and T = temperature. The process was repeated for 5000 cycles. In addition to the cycles of attempted torsional rotations and energy minimizations, the system was periodically subjected to a simulated annealing protocol in an attempt to avoid the conformation getting stuck in a local minimum. To simulate the effects of solvation and to reduce computational overheads, a distance-dependent dielectric term was used to simulate the electrostatic energy component. Each pair of modules was found to rapidly converge to a single energy minimum, representing a stable conformation. These were then used, in conjunction with the crystal structure of CCP 1 and 2, to create a model for the structure of the four CCPs of MCP.

²J. Parkinson, P. N. Barlow, and J. P. Atkinson, unpublished observation.

		Residues										
A.	MCP	N	E	G	Y	Y	L	I	G	E	E	94–103
	C4BP, human	S	—	—	F	F	—	—	—	S	T	141–150
	C4BP, bovine	S	—	—	—	V	—	—	—	S	A	140–149
	C4BP, rabbit	S	—	—	—	I	—	—	—	S	T	140–149
	C4BP, rat	S	—	—	—	I	—	—	—	S	S	104–114
B.	MCP	W	S	G	K	P	P	I	C			116–123
	CR1, human	—	—	T	—	—	—	—	—			604–611
		—	—	T	—	—	—	—	—			1054–1061
	CR1, chimp	—	—	T	—	—	—	—	—			579–586
		—	—	T	—	—	—	—	—			1029–1036
	CR1, baboon	—	—	T	—	—	—	—	—			491–498
		—	—	T	—	—	—	—	—			941–948

FIG. 3. Ligand-interacting peptides of human MCP show homologies to C4BP (A) and CR1 (B) of several species. These two peptide homologies were identified by a BLAST search of the National Center for Biotechnology data base (35).

RESULTS

Table I presents the sequence of mutants investigated for functional activity.

Carboxyl-terminal Segment of CCP 1 Is Important for C4b Binding—In prior studies, deletion of CCP 1 had no effect on C3b binding or CA (21, 22) but reduced C4b binding (21). CCP 1 is also required for MV binding (22–26) and, in particular, amino acids 47–61 were involved in recognition by MV hemagglutinin (24). Complement-related functional analysis of this same mutant (residues 47–61) revealed decreased C4b binding and CA (Table II). C3b binding and CA were not altered. Thus, these data map a region specific for a C4b interaction to the carboxyl terminus of CCP 1, a site that overlaps with one required for binding to MV hemagglutinin.

Overlapping Peptides Disclose Functional Sites—To further analyze the carboxyl terminus of CCP 1 as well as all of CCP 2, an ELISA format was used to assess ligand binding of overlapping MCP peptides (Fig. 1). In this screening assay, C4b binding by peptides 14 and 15 in CCP 1 and peptides 23 and 29 in CCP 2 was reproducibly observed at 3–4-fold over background or relative to peptides 16–21 (Fig. 2). Peptide 22 and peptides between 23 and 29 demonstrated intermediate levels of binding reflecting, in part, the overlap with peptides 23 and 29. Peptides 14 and 15 contain the same region of CCP 1 as noted in

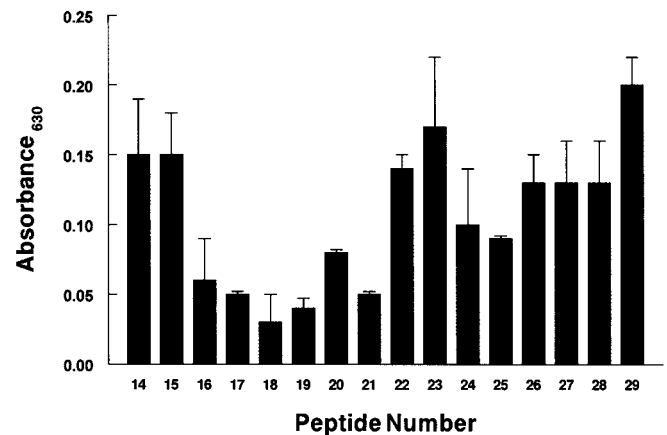


FIG. 2. Binding of MCP peptides to C4b. Overlapping peptides in CCP 1 and 2 (see Fig. 1) were coated on microtiter plates and C4b binding monitored in an ELISA in three separate experiments.

the preceding analysis (*i.e.* mutant 47–61), providing further evidence that this region is involved in C4b binding.

With these ELISA data as a starting point, mutants were next constructed substituting alanines for residues within peptides 23 and 29 of CCP 2 (Table II) that possessed high homology to C4BP (residues 94–103) or to CR1 (residues 118–122) (Fig. 3). These two regions were identified by a BLAST search of peptides 23 and 29 in the National Center for Biotechnology data base (35). For the first set (94–103), single mutants demonstrated variable decreases in C4b CA (Table II). For several (Y97A, Y98A, L99A, and E103A), there were substantial decreases in CA but minimal or no change in C4b binding. In contrast, C4b binding and CA were diminished in mutants N94A, E95A, G96A, and E102A. Interestingly, the peptide NEGYYLIGEE is contained within one that almost completely inhibited MV binding and infection in CCP 2 (*i.e.* FGYQMH-FICNEGYYLIGEEI (Ref. 24)). This same region has been implicated in MV binding by multiple groups (24, 25, 27, 36, 37). Thus, these results point to a second site in MCP, encompassing amino acids 94–103, important for both C4b and MV interactions.

The next area explored was based on the increased binding of peptide 29 to C4b. Amino acids 118–122 were each substituted with an alanine. These five mutants retained C3b and C4b binding similar to wild type, although the 120–122 mutants were less efficient in C4b CA (Table II). These data suggest that residues near the fourth Cys of CCP 2 are involved in C4b CA and are consistent with prior findings in which MCP with CCP 2 deleted bound C3b and C4b but lacked CA (21).

Indel in CCP 3 Is a Functional Site—Indels (*i.e.* amino acid

insertions or deletions producing length polymorphisms among members of a protein family) are good candidates for protein: protein interactive sites (38). Following Cys-2 in CCP 3 is a peptide insertion of eight amino acids (amino acids 158–165; sequence DPAPGPDP). Alanine substitutions produced three mutants (P161A, G162A/P163A, and D164A/P165A) with undetectable or diminished C3b and C4b CA but no or more limited decreases in ligand binding (Table III). Most striking was mutant P161A that lacked C3b CA and had minimal C4b CA but largely retained ligand binding capability.

Sequence and Functional Comparisons of Primate MCPs—We next compared ligand binding of human and non-human primate MCP (Fig. 4). Consistent with previous data, human MCP (from a CHO transfectant) bound C4b more efficiently than C3b (39). Gorilla erythrocytes did not bind C3b or C4b because they do not express MCP on this cell type (29, 40). The orangutan binding pattern was similar to humans. How-

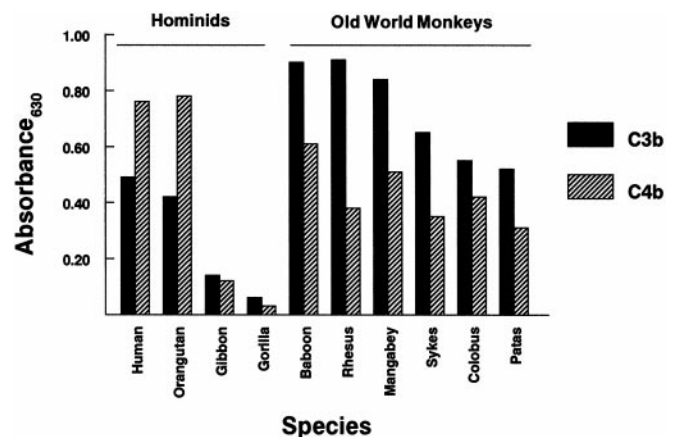


FIG. 4. Comparison of human and primate MCP binding of human C3b and C4b. Solubilized primate erythrocytes and CHO human MCP transfectant lysate (1×10^9 MCP molecules) were compared in an ELISA format in which C3b or C4b was coated on wells. A representative experiment of three is shown. Gorilla erythrocytes do not express MCP (29, 40) and, therefore, serve as a negative control for these experiments (using the highest number of erythrocyte cell equivalents). Gibbons express MCP on erythrocytes in similar quantities to orangutan, but bind human C3b and C4b poorly.

TABLE III

Functional consequences of alanine mutations in the indel of CCP 3
Functional assessments as per Table II.

Mutant	C3b		C4b	
	Binding	Cofactor	Binding	Cofactor
	%		%	
D158A/P159A	110	++++	107	+++
P161A	83	—	80	+
G162A/P163A	76	++	89	++
D164A/P165A	61	++	89	++

CCP 2

Human ⁶⁴TCPYIRDPLN GQAVPANGTY EFGYQMHFIC NEGYYLIGEE ILYCELKGSV AIWSGKPPIC EKV¹²⁶
 Baboon M--H-Q--V- -E-ILV--S- ---SEL--- -----KD -----DT- -----L- --I
 Rhesus M--H----- -E-IL---S- ---AEL--- -----KD -----DT- -----L- --I
 Primate A Primate B

CCP 3

Human ¹²⁷LCTPPPKIKN GKHTFSEVEV FEYLDVAVTYS CDPAPGPDPF SLIGESTIYC GDNSVWSRAA PECKVV¹⁹²
 Baboon ----- -R----- -----M--- -N--T-H--- -----
 Rhesus ----- ----- -----M--- -N--T-H--- -----
 Primate C

CCP 4

Human ¹⁹³KCRFPVVEVNG KQISGFQKGF YYKATVMFEC DKGFYLDGSD TIVCDNSNTW DPPVPKCLK²⁵¹
 Baboon ----- ----- ---Y--N--- K---E----- -----
 Rhesus ----- ----- ---Y--N--- K---E----- -----
 Primate D

FIG. 5. Comparison of amino acid sequences of human, baboon, and rhesus MCP. Identical amino acids are indicated by a dash. Those that differ from the human sequence are indicated. Primate residues substituted into the human sequence are noted as "Primate" mutants A–D (see Table I).

ever, the six Old World monkeys bound C3b more efficiently than C4b. Of these, the sequence of MCP is available for baboon and rhesus (Fig. 5). We asked if these sequence differences enhanced C3b binding and/or diminished C4b binding to account for this pattern reversal. Constructs were prepared in which selected primate sequences were substituted in human MCP (Fig. 5). Two of these mutants showed elevated binding selectively to C3b (*i.e.* primate A and D) as well as enhanced C3b CA (Table IV). These gain-of-function mutants suggest that an increase in the affinity of MCP for C3b accounted for the binding results presented in Fig. 3 and that these two regions (A and D) are involved in C3b interactions.

Block Peptide and Individual Amino Acid Substitutions in CCP 3 and 4—DAF is a closely related, structurally similar RCA protein that possesses four CCPs as well as an STP region (reviewed in Ref. 41). Because CCP 1 of DAF does not possess complement regulatory function (42), segments of DAF CCP 1 were substituted in homologous regions of MCP CCP 3 or 4. Of 16 such block substitutions, six were expressed similar to wild

type and functionally assessed (Table V). Mutant 151–158 demonstrated no alteration in function while two mutants, 183–190 and 243–250, lost activity. Mutants 193–197 and 205–212 exhibited partial decreases in ligand binding with corresponding decreases in CA. In contrast, mutant 127–134 demonstrated no change in ligand binding, yet C3b CA was abrogated and C4b CA reduced by ~50%.

To identify the functionally important amino acids within these block substitutions, individual residues were substituted with an alanine or with the corresponding amino acids from DAF (Table V). Within the series 127–134, T129A/P130A accounted for the decrease in C4b function and partially for diminished C3b function. In the segment 183–191, individual mutants S183T and R184K had no effect while mutants A185I, E188F, and V191D demonstrated partial decreases in function, especially CA. These results suggest that the region immediately surrounding the fourth cysteine in CCP 3 is involved in both C3b and C4b binding.

In the case of individual mutations within 193–197 and

TABLE IV
Functional analysis of mutants with primate to human amino acid interchanges

Functional assessments are per Table II.

Mutant	CCP	C3b		C4b	
		Binding	Cofactor	Binding	Cofactor
		%		%	
Primate A (E102K/E103D/G111D/S112T)	2	118	+++++ ^a	102	++++
Primate B (I122L/V126I)	2	97	++++	101	++++
Primate C (T174M/D179N/V182T/S184H)	3	110	++++	102	++++
Primate D (F226Y/D229N/T233K)	4	129	+++++	95	++++

^a +++++, indicates >120% of wild type.

TABLE V
Functional effects of amino acid substitutions in CCP 3 and 4

Mutants described in Table I and functional assessments per Table II.

Mutant	CCP	C3b		C4b	
		Binding	Cofactor	Binding	Cofactor
		%		%	
127–134 ^a	3	97	–	93	++
T129A/P130A	3	71	++	78	++
I134A	3	110	+++	105	+++
151–158	3	110	++++	90	++++
183–190 ^b	3	1	–	5	–
S183T	3	86	++++	101	++++
R184K	3	91	++++	115	++++
A185I	3	112	++++	107	++
E188F	3	68	++	58	–
V191D	3	44	++	42	++
193–197	4	33	–	55	++
K193A	4	37	–	100	++
R195A	4	50	+	100	++
F196A	4	35	–	99	+
P197A	4	100	+	100	+
205–212	4	75	–	55	++
I205A	4	116	+	98	+++
S206A	4	103	+	107	++
G207A	4	71	–	78	++
F208A	4	30	–	99	+
G209A	4	114	+	99	+
K210A	4	68	+	113	+++
K211A	4	56	–	94	++
F212A	4	32	–	120	++
243–250	4	6	–	7	–
D243A	4	98	++++	79	+++
P244A	4	106	++++	104	++
P245A	4	92	++	80	+++
V246A	4	103	++	104	+++

^a Hyphenated mutant numbers indicate a block of MCP amino acids substituted with the homologous region of CCP 1 of human DAF (see Table I).

^b Amino acids 186, 187, and 189 are identical in DAF and mutant K190A was not expressed.

TABLE VI

Binding of a function-blocking mAb to selected mutants

Mutants are listed in Table I.

Mutant	GB24 binding ^a
R-CHO	— ^b
MCP	++++
CCP 3	
T129A/P130A	++++
P161A	++++
G162A/P163A	++++
D164A/P165A	—
183–190	++++
CCP 4	
193–197	—
K193A	++++
R195A	+++
F196A	—
P197A	+++
205–212	—
I205A	++++
S206A	++++
G207A	++
F208A	—
G209A	++++
K210A	++++
K211A	++++
F212A	++++
243–250	—
D243A	++++
P244A	++++
P245A	++++
V246A	++++

^a None of these mutations altered binding to mAb TRA-2–10.^b — is ≤10% of wild-type MCP binding; ++, 40–69%; +++, 70–90%; +++++, 91–100%.

205–212, most had functional alterations of nearly the same magnitude as those of the parental protein. Additionally, while mutant 243–250 lacked activity, none of the individual mutants in peptide 243–246 accounted for the loss of activity, although several (P244A, P245A, and V246A) did show diminished cofactor function.

Epitope Mapping of a Function Blocking mAb—The mAb to MCP, GB24, blocks C3b and C4b binding and interacts with an epitope that requires the presence of CCP 3 and 4 (21). We compared the binding of GB24 to selected mutants of CCP 3 and CCP 4 in parallel with a non-function blocking antibody, TRA-2–10, that binds to CCP 1 (23). All mutants bound similarly to TRA-2–10 (data not shown). In CCP 3, GB24 did not bind to the double mutant D164A/P165A (Table VI). This same mutant had significantly reduced functional activity (Table III) and is part of the indel in CCP 3. For CCP 4, three block substitution mutants also abrogated binding by GB24. These same mutants were functionally deficient (see Table V). Within these blocks, alanine substitutions indicated that amino acids Phe¹⁹⁶, Gly²⁰⁷, and Phe²⁰⁸ were critical for GB24 binding. Although the block substitution mutant (243–250) lost reactivity to GB24, individual mutants in peptide 243–246 did not show a loss of binding.

Structural Analysis of MCP—Electrostatic depiction (Fig. 6) of the modeled structure reveals the surface to be mainly negatively charged with a single large patch of positive charges located over the “front” face that spans the junction between modules 3 and 4. The latter is a site identified by mutagenesis (Table V) as important for C3b binding. Decreasing the positive charge in this region (K193A, R195A, K210A, K211A) inhibited C3b binding. In contrast, substituting a similarly charged residue (R184K) did not alter function. Additionally, two sites for C4b interaction that overlap with MV binding regions in CCP 1 and 2 (shown on Fig. 6) lie within primarily negatively

charged areas. In this region of CCP 2, a reduction in negative charge (E95A, E102A, and E103A) decreased primarily C4b CA (Table II).

Finally, residues involved in binding of mAb GB24, which also were important for both C3b and C4b function, map to two areas that lie close to each other on the same face (Asp¹⁶⁴/Pro¹⁶⁵, Phe¹⁹⁶, Gly²⁰⁶, and Phe²⁰⁸).

Structural Interpretation of Mutational Analyses of MCP—Fig. 7A reveals the same large patch of positively charged residues implicated in C3b binding located on or close to the “front” face of the 3/4 junction in Fig. 6. Other residues implicated in C3b binding (Glu¹⁰², Glu¹⁸⁸, and Val¹⁹¹) are located on the opposite face of the modeled structure. Of the primate-interchange CCP 4 mutation (T233K, D229N, and F226Y) that increased C3b binding activity, Thr²³³ is in close proximity to the positively charged surface patch.

Residues implicated in C4b binding are located in several regions of the modeled structure. A patch of residues lies on the front face close to the 2/3 interface. The positions of other residues appear to be dispersed over the surface of the structure and are necessary for both C4b and C3b binding.

Fig. 7B shows the positions of residues implicated in CA. Multiple residues that affected mainly C4b CA are close to the putative C3b binding positively charged patch at the 3/4 junction. Another site for C4b CA is located close to the putative C4b binding site at the 2/3 junction. The few amino acids exclusively influencing C3b CA were on the back side of the C3b binding area in CCP 4.

DISCUSSION

The purpose of the present study was to delineate complement regulatory sites within the four CCP modules of MCP. Earlier studies demonstrated that CCPs 2, 3, and 4 were most important for ligand binding and CA (21, 22). We have now obtained further data relative to the structure and regulatory function of MCP. First, regions that participate in complement inhibitory activity were identified in each of the four CCPs. Second, although many mutations produced changes in both C4b and C3b binding, others produced a selective alteration, suggesting overlapping as well as distinct requirements for these two ligands. Third, a reduction in ligand binding produced a proportional decrease in CA; however, the reverse was not true as other mutants possessed ligand binding activity similar to wild type, while CA was reduced or abrogated. Fourth, CA for C3b and C4b also was separable as indicated by mutants that lost CA for one or the other ligand. Fifth, we have produced a model of four repeats of MCP and analyzed the mutagenesis results in light of this proposed structure.

Nine regions likely to be involved in complement inhibition are highlighted in Fig. 8. Eight of these areas are adjacent to or incorporate a cysteine. Three regions, two in CCP 3 and one in CCP 4, are proline-rich, each having at least three prolines in a stretch of ≤5 amino acids. No other such proline-rich sequences are found in the CCPs of MCP. A comparison of Fig. 8A with Fig. 8B suggests that these prolines are part of protruding loops and strands. A site at the carboxyl terminus of each module, encompassing the fourth cysteine, was involved in functional activity. Substitutions in this region in CCPs 1 and 2 influenced only C4b CA while in CCPs 3 and 4 altered both C4b and C3b interactions. A mutated site near the first Cys of CCP 3 and 4 reduced both C3b and C4b interactions. These observations are consistent with ligand contact points occurring at the junction between modules or with amino acid changes at this site influencing the spatial relationships between modules. Additionally, residues likely to be important for C4b and C3b interactions are located after the second Cys in CCPs 2 and 3. The region in CCP 3 possesses four prolines and

FIG. 6. **Electrostatic model of MCP showing front (left) and back (right) views.** Yellow (GB24 binding), green (measles virus binding), and light blue (C4b binding) indicate putative interactive sites.

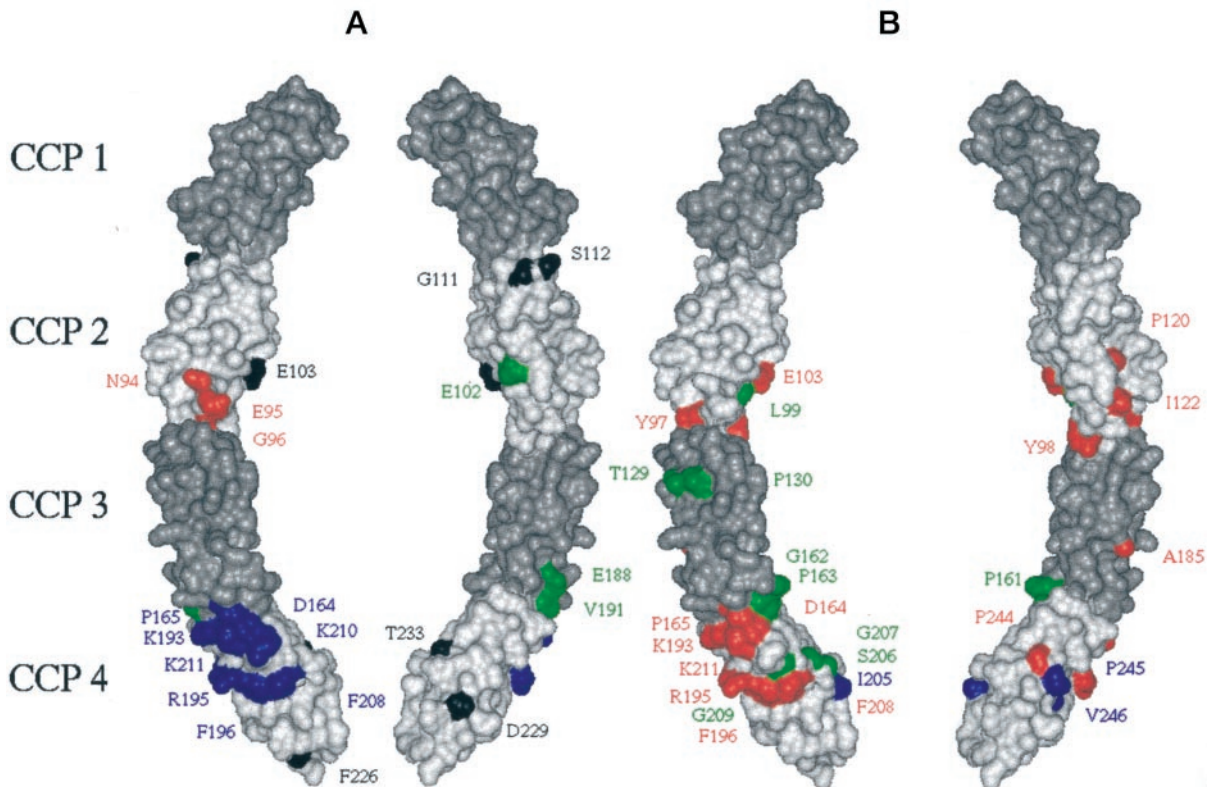
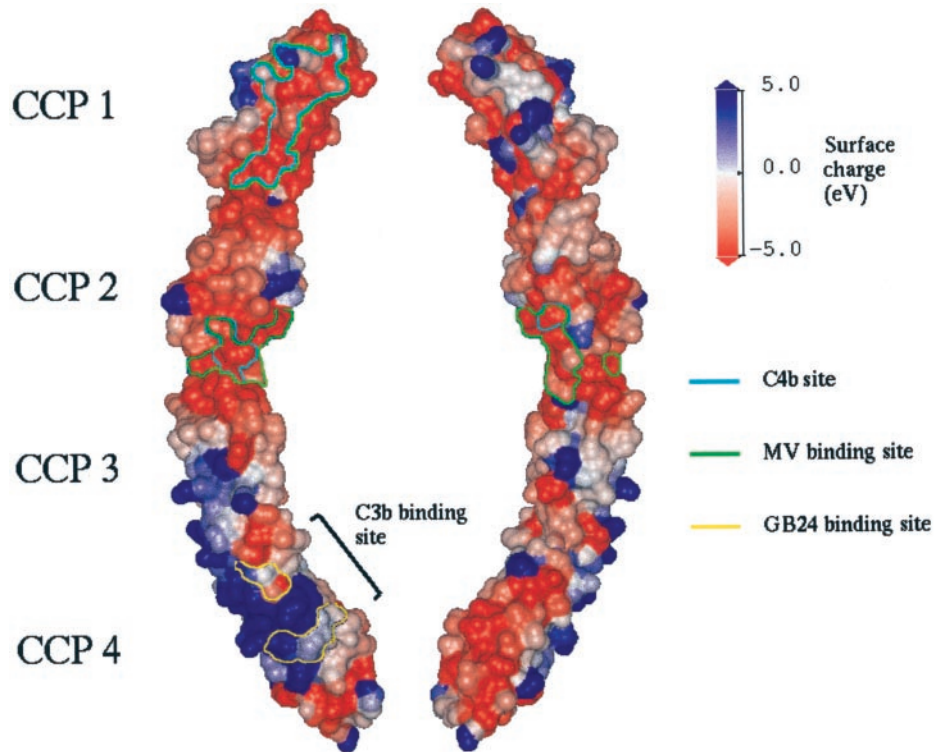


FIG. 7. **Model of MCP functional sites.** A, front (left) and back (right) views of CCPs 1–4 indicating binding sites for C3b and C4b. B, front and back views of CCPs 1–4 indicating CA sites for C3b and C4b. Colors for ligands: blue, C3b; red, C4b; green, both C3b and C4b; black, increased C3b binding and CA.

overlaps with the indel. Of interest, a similar indel is present in three highly homologous and functionally important CCPs (3, 10, and 17) of CR1 (43).

We identified two C4b-regulatory sites that had been previously characterized as MV interactive regions (Figs. 6 and 8). CCPs 1 and 2 (including the *N*-glycosylation site of CCP 2 (see

Refs. 24 and 44–46)) are involved in MV binding and infection, especially between residues 37–56 in CCP 1 and 85–106 in CCP 2 (22–26, 36, 37). Recently, Casanovas *et al.* (27) ascertained the crystal structure at 3.1-Å resolution of CCPs 1 and 2. They proposed that MCP residues 94–97 in CCP 2 make direct contact with the virus. Thus, MV hemagglutinin appears to

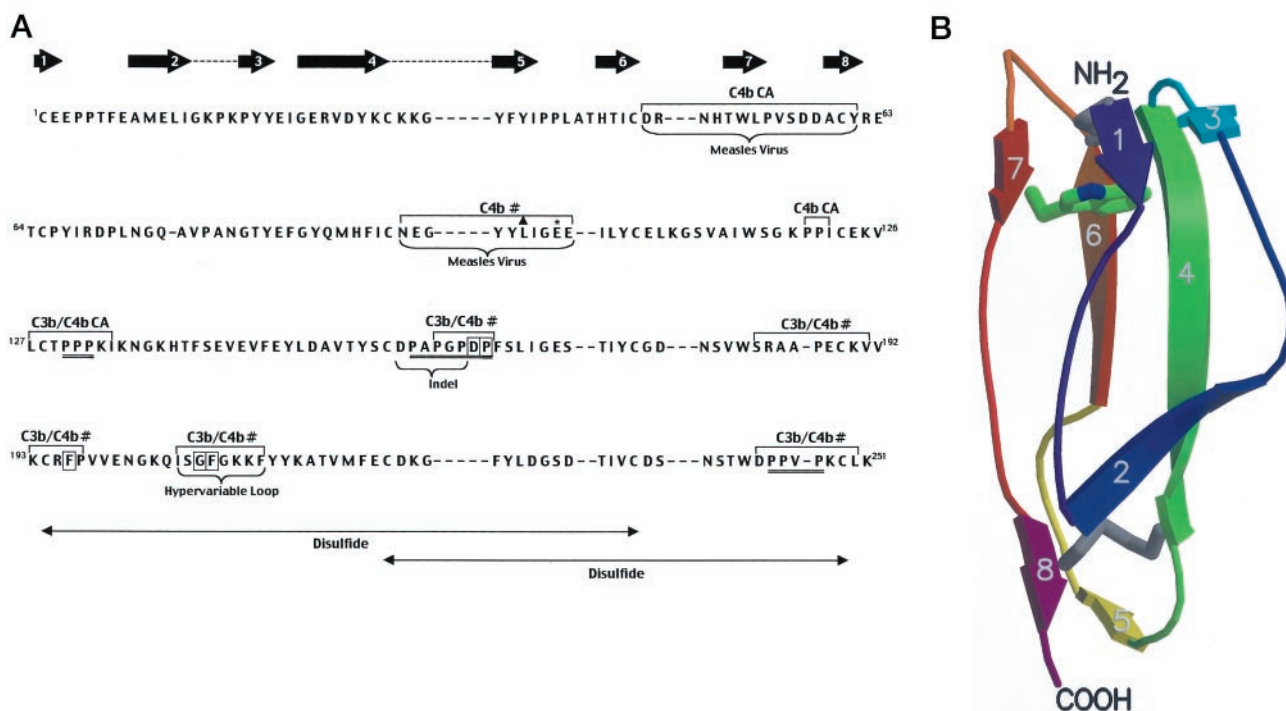


FIG. 8. A, proposed complement regulatory sites of MCP. The sequence of the four CCPs is shown. Areas of β -sheets are presented as arrows above CCP-1. Dashed lines between 2 and 3 as well as 4 and 5 indicate plasticity in length of these loops. Putative regulatory regions are noted in brackets above the sequence. Boxed residues are those, if mutated, led to a loss of binding by function-blocking mAb, GB24. Proline-rich areas are double-underlined. CA, cofactor activity; #, these sites show mixed functions (*i.e.* binding and/or CA); ▲, Leu⁹⁹, also important for C3b binding. B, model of CCP 1 of MCP generated by Molscript (67). β -Sheets are numbered, disulfide bonds at each terminus (between β -sheets 4 and 8; and 1 and 6) are depicted. The highly conserved tryptophan (green ring) is shown with its blue nitrogen group.

dock to a functionally important site for C4b complement regulation in both CCP 1 and CCP 2. A structural relationship between C4b and hemagglutinin is suggested by these results. Interestingly, new world primates delete CCP 1 by alternative splicing, a change preventing MV binding (26). The functional consequence of this change may be tolerated because C3b regulatory activity is minimally altered and there is retention, albeit less efficient, of C4b regulatory activity.

Since CCPs share a similar overall structure, it is reasonable to propose common functional sites in such proteins (47, 48). For example, each CCP has a hydrophobic core interlaced with β -strands accompanied by protruding loops. The latter, as already pointed out, are strong candidates for functional sites (49). One such area with a variable length and sequence has been termed the "hypervariable loop" (47–50). Block and individual substitutions within this loop influenced both C3b and C4b interactions. This region also is part of the epitope for the function-blocking MCP mAb, GB24, and is important for C3b/C4b interactions in CCPs 8 and 10 of CR1 (43). Another such comparison among MCP, C4BP, and CR1 centers on the first Cys of a CCP. In the case of MCP, functional sites were suggested in CCP 3 and 4 near Cys 1 (*i.e.* amino acid series 127–134 and 193–197; and Phe¹⁹⁶ for GB24 binding). Likewise, residues near Cys 1 in CCP 2 of C4BP are critical for C4b binding (51) and in CCP 2 of CR1 for C3b and C4b interactions (43). MCP residues surrounding the fourth Cys of CCPs 1–4 were found to be important for C4b regulatory activity and in CCP 3 and 4 for C3b. This area corresponds in CR1 (CCPs 9 and 16) to a site important for C3b binding and CA (43). Finally, as shown in Fig. 3, there are two highly homologous regions to MCP in C4BP and CR1. These regions are ones likely to be involved in C4b regulation as they are in MCP (52).

The structures of four CCP-containing proteins have been determined (factor H, 15–16 (Ref. 48)); vaccinia virus complement control protein, 2–4 (Refs. 53 and 54); β -glycoprotein, 1–5

(Refs. 55 and 56); and MCP, 1–2 (Ref. 27)). For each, the modules aligned in an end-to-end fashion, sharing a relatively small interface. Results from the simulations performed here suggest that MCP modules are also joined end-to-end leading to the formation of an extended structure (Figs. 6 and 7). As with the known structures, the intermodular junctions between MCP 2/3 and MCP 3/4 appear to be limited and dominated by hydrophobic interactions.³

RCA proteins interact with components of complement in an ionic strength dependent manner (57, 58) and the charge characteristics of the amino terminus of the α -chains of C3b and C4b are predicted to be conserved (59–63). The functional role of the positively charged surface patch of residues in modules 3 and 4 (Fig. 6) supports this hypothesis. Mutations decreasing the magnitude of this charge produced a decrease in C3b binding. The mutation T233K (located close to this patch) would increase the magnitude of positive charge and may be in part responsible for the increase in C3b binding activity associated with the triple primate mutant F226Y/D229N/T233K. In contrast, the data suggest a more critical role for negatively charged residues in C4b interactions.

Regarding C4b interactions (Table II and Fig. 7), Gly⁹⁶ specifically affects C4b binding and is located close to residues thought to be important in forming direct interactions with ligand (*i.e.* loop with Asn⁹⁴/Glu⁹⁵). Substitution of several residues close to the junction of CCP 2/3 (Tyr⁹⁷, Tyr⁹⁸, Leu⁹⁹, Glu¹⁰³, Ile¹²²) altered C4b CA. The lack of effect of the mutations Y97A and Y98A on other functionalities suggests that they do not lead to a change in junctional contacts. Given that neither of these residues is surface exposed, we postulate that, after binding C4b, the 2/3 junction alters in such a way so as to expose these two residues for interaction with the C4b/factor I

³ J. Parkinson, M. K. Liszewski, P. N. Barlow, and J. P. Atkinson, unpublished observation.

complex. The surface exposed residues, Leu⁹⁹, Glu¹⁰³, and Ile¹²², may also be involved in forming direct interactions with the cofactor complex.

In summary, these mutagenesis and modeling data represent the initial analysis of ligand binding and cofactor sites within the CCPs of MCP. An issue common to structure-function analyses by mutagenesis is whether a conformational change is responsible for the altered activity. Resolving this issue requires a three dimensional structure of the binding site with its attached ligand. Thus, our future plans include elucidating intermolecular junctions and determination of the three-dimensional structure of CCPs 3 and 4 by physicochemical studies and NMR spectroscopy as we have begun to do for the active sites of CR1 (64–66). Informative comparisons to other C3b/C4b binding proteins will be possible as will further interpretations of the mutagenesis results. A structural analysis of the interactions of MCP with its natural *versus* pathogenic ligands should have important implications for understanding complement inhibition and microbial pathogenesis.

Acknowledgments—We thank Dennis Hourcade, Richard Hauhart and Malgorzata Krych-Goldberg for their review of the manuscript, and Madonna Bogacki and Lorraine Whiteley for editorial assistance.

REFERENCES

- Liszewski, M. K., Farries, T. C., Lublin, D. M., Rooney, I. A., and Atkinson, J. P. (1996) *Adv. Immunol.* **61**, 201–283
- Naniche, D., Varior-Krishnan, G., Cervoni, F., Wild, T. F., Rossi, B., Rabourdin-Combe, C., and Gerlier, D. (1993) *J. Virol.* **67**, 6025–6032
- Dorig, R. E., Marcil, A., Chopra, A., and Richardson, C. D. (1993) *Cell* **75**, 295–305
- Manchester, M., Liszewski, M. K., Atkinson, J. P., and Oldstone, M. B. A. (1994) *Proc. Natl. Acad. Sci. U. S. A.* **91**, 2161–2165
- Okada, N., Liszewski, M. K., Atkinson, J. P., and Caparon, M. (1995) *Proc. Natl. Acad. Sci. U. S. A.* **92**, 2489–2493
- Kallstrom, H., Liszewski, M. K., Atkinson, J. P., and Jonsson, A.-B. (1997) *Mol. Microbiol.* **25**, 639–647
- Santoro, F., Kennedy, P. E., Locatelli, G., Malnati, M. S., and Berger, E. A. (1999) *Cell* **99**, 817–827
- Howard, J., Justus, D. E., Totmenin, A. V., Shchelkunov, S., and Kotwal, G. J. (1998) *J. Leukocyte Biol.* **64**, 68–71
- Lozahic, S., Christiansen, D., Manie, S., Gerlier, D., Billard, M., Boucheix, C., and Rubinstein, E. (2000) *Eur. J. Immunol.* **30**, 900–907
- Cervoni, F., Oglesby, T. J., Adams, E. M., Milesi-Fluet, C., Nickells, M. W., Fenichel, P., Atkinson, J. P., and Hsi, B. L. (1992) *J. Immunol.* **148**, 1431–1437
- Xu, C., Mao, D., Holers, V. M., Palanca, B., Cheng, A. M., and Molina, H. (2000) *Science* **287**, 498–501
- Seya, T., Hara, T., and Matsumoto, M. (1993) *Eur. J. Immunol.* **23**, 1322–1327
- Anderson, D. J., Michaelson, J. S., and Johnson, P. M. (1989) *Biol. Reprod.* **41**, 285–293
- Anderson, D. J., Abbott, A. F., and Jack, R. M. (1993) *Proc. Natl. Acad. Sci. U. S. A.* **90**, 10051–10055
- Kitamura, M., Matsumiya, K., Yamanaka, M., Takahara, S., Hara, T., Matsumoto, M., Namiki, M., Okuyama, A., and Seya, T. (1997) *J. Reprod. Immunol.* **33**, 83–88
- Higgins, P. J., Ko, J.-L., Lobell, R., Sardonini, C., Alexki, M. K., and Yeh, C. G. (1997) *J. Immunol.* **158**, 2872–2881
- Rooney, I. A., Liszewski, M. K., and Atkinson, J. P. (1993) *Xeno* **1**, 29–35
- Cozzi, E., and White, D. J. G. (1995) *Nat. Med.* **1**, 964–966
- Post, T. W., Liszewski, M. K., Adams, E. M., Tedja, I., Miller, E. A., and Atkinson, J. P. (1991) *J. Exp. Med.* **174**, 93–102
- Russell, S. M., Sparrow, R. L., McKenzie, I. F. C., and Purcell, D. F. J. (1992) *Eur. J. Immunol.* **22**, 1513–1518
- Adams, E. M., Brown, M. C., Nunge, M., Krych, M., and Atkinson, J. P. (1991) *J. Immunol.* **147**, 3005–3011
- Iwata, K., Seya, T., Yanagi, Y., Pesando, J. M., Johnson, P. M., Okabe, M., Ueda, S., Ariga, H., and Nagasawa, S. (1995) *J. Biol. Chem.* **270**, 15148–15152
- Manchester, M., Valsamakis, A., Kaufman, R., Liszewski, M. K., Alvarez, J., Atkinson, J. P., Lublin, D. M., and Oldstone, M. B. A. (1995) *Proc. Natl. Acad. Sci. U. S. A.* **92**, 2303–2307
- Manchester, M., Gairin, J. E., Alvarez, J., Liszewski, M. K., Atkinson, J. P., and Oldstone, M. B. A. (1997) *Virology* **233**, 174–187
- Buchholz, C. J., Koller, D., Devaux, P., Mumenthaler, C., Schneider-Schaulies, J., Braun, W., Gerlier, D., and Cattaneo, R. (1997) *J. Biol. Chem.* **272**, 22072–22079
- Hsu, E. C., Dorig, R. E., Sarangi, F., Marcil, A., Iorio, C., and Richardson, C. D. (1997) *J. Virol.* **71**, 6144–6154
- Casasnovas, J. M., Larvie, M., and Stehle, T. (1999) *EMBO J.* **18**, 2911–2922
- Liszewski, M. K., Leung, M. K., and Atkinson, J. P. (1998) *J. Immunol.* **161**, 3711–3718
- Nickells, M. W., Subramanian, V. B., Clemenza, L., and Atkinson, J. P. (1995) *J. Immunol.* **154**, 2829–2837
- Andrews, P. W., Knowles, B. B., Parkar, M., Pym, B., Stanley, K., and Goodfellow, P. N. (1985) *Ann. Hum. Genet.* **49**, 31–39
- Hsi, B. L., Yeh, C.-J. G., Fenichel, P., Samson, M., and Grivaux, C. (1988) *Am. J. Reprod. Immunol. Microbiol.* **18**, 21–27
- Sali, A., and Blundell, T. (1993) *J. Mol. Biol.* **234**, 779–815
- Brunger, A. (1992) *X-PLOR Version 3.1: A System for X-ray Crystallography and NMR*, Yale University Press, New Haven
- MacKerell, A. D., Bashford, D., Bellott, M., Dunbrack, R. L., Evanseck, J. D., Field, M. J., Fischer, S., Gao, J., Guo, H., Ha, S., McCarthy, D., Kuchnir, L., Kuczera, K., Lau, F. T. K., Mattos, C., Michnick, S., Ngo, T., Nguyen, D. T., Prodhom, B., Reiher, W. E., Roux, B., Schlenkrich, M., Smith, J. C., Stote, R., Straub, J., Watanabe, M., Wiorkiewicz-Kuczera, J., Yin, D., and Karplus, M. (1998) *J. Phys. Chem. B* **102**, 3586–3616
- Altschul, S. F., Gish, W., Miller, W., Myers, E. W., and Lipman, D. J. (1990) *J. Mol. Biol.* **215**, 403–410
- Mumenthaler, C., Schneider, U., Buchholz, C. J., Koller, D., Braun, W., and Cattaneo, R. (1997) *Protein Sci.* **6**, 588–597
- Hsu, E. C., Sabatinos, S., Hoedemaeker, F. J., Rose, D. R., and Richardson, C. D. (1999) *Virology* **258**, 314–326
- Ogata, R. T., Ai, R., and Low, P. J. (1998) *J. Immunol.* **161**, 4785–4794
- Liszewski, M. K., and Atkinson, J. P. (1996) *J. Immunol.* **156**, 4415–4421
- Nickells, M. W., and Atkinson, J. P. (1990) *J. Immunol.* **144**, 4262–4268
- Liszewski, M. K., and Atkinson, J. P. (1998) in *The Complement System* (Rother, K., Till, G. O., and Hansch, G. M., eds) pp. 146–162, Springer-Verlag, Berlin
- Coyne, K. E., Hall, S. E., Thompson, E. S., Arce, M. A., Kinoshita, T., Fujita, T., Anstee, D. J., Rosse, W., and Lublin, D. M. (1992) *J. Immunol.* **149**, 2906–2913
- Krych, M., Hauhart, R., and Atkinson, J. P. (1998) *J. Biol. Chem.* **273**, 8623–8629
- Maisner, A., Schneider-Schaulies, J., Liszewski, M. K., Atkinson, J. P., and Herrler, G. (1994) *J. Virol.* **68**, 6299–6304
- Maisner, A., and Herrler, G. (1995) *Virology* **210**, 479–481
- Maisner, A., Alvarez, J., Liszewski, M. K., Atkinson, J. P., Atkinson, D., and Herrler, G. (1996) *J. Virol.* **70**, 4973–4977
- Barlow, P. N., Norman, D. G., Steinkasserer, A., Horne, T. J., Pearce, J., Driscoll, P., Sim, R. B., and Campbell, I. D. (1992) *Biochemistry* **31**, 3626–3634
- Barlow, P. N., Steinkasserer, A., Norman, D. G., Kieffer, B., Wiles, A. P., Sim, R. B., and Campbell, I. D. (1993) *J. Mol. Biol.* **232**, 268–284
- Perkins, S. J., Harris, P. I., Sim, R. B., and Chapman, D. (1988) *Biochemistry* **27**, 4004–4012
- Baron, M., Norman, D. G., and Campbell, I. D. (1994) *Trends Biochem. Sci.* **16**, 13–17
- Accardo, P., Sanchez-Corral, P., Criado, O., Garcia, E., and Rodriguez de Cordoba, S. (1996) *J. Immunol.* **157**, 4935–4939
- Krych-Goldberg, M., Hauhart, R. E., Bala Subramanian, V., Yurcisin, B. M., II, Crimmins, D. L., Hourcade, D. E., and Atkinson, J. P. (1999) *J. Biol. Chem.* **274**, 31160–31168
- Kirkitaadze, M. D., Henderson, C., Price, N. C., Kelly, S. M., Mullin, N. P., Parkinson, J., Dryden, D. T. F., and Barlow, P. N. (1999) *Biochem. J.* **344**, 167–175
- Wiles, A. P., Shaw, G., Bright, J., Perczel, A., Campbell, I. D., and Barlow, P. N. (1997) *J. Mol. Biol.* **272**, 253–265
- Schwarzenbacher, R., Zeth, K., Diederichs, K., Gries, A., Kostner, G. M., Laggner, P., and Prassl, R. (1999) *EMBO J.* **18**, 6228–6239
- Bouma, B., de Groot, P. G., van den Elsen, J. M. H., Ravelli, R. B. G., Schouten, A., Simmelink, M. J. A., Derksen, R. H. W. M., Kroon, J., and Gros, P. (1999) *EMBO J.* **18**, 5166–5174
- Cole, J. L., Housley, G. A., Jr., Dykman, T. R., MacDermott, R. P., and Atkinson, J. P. (1985) *Proc. Natl. Acad. Sci. U. S. A.* **82**, 859–863
- Dykman, T. R., Cole, J. L., Iida, K., and Atkinson, J. P. (1983) *Proc. Natl. Acad. Sci. U. S. A.* **80**, 1698–1702
- Taniguchi-Sidle, A., and Isenman, D. E. (1994) *J. Immunol.* **153**, 5285–5302
- Oran, A. E., and Isenman, D. E. (1999) *J. Biol. Chem.* **274**, 5120–5130
- Lambris, J. D., Loa, Z., Oglesby, T. J., Atkinson, J. P., Hack, C. E., and Becherer, J. D. (1996) *J. Immunol.* **156**, 4821–4832
- Barlow, P. N., Baron, M., Norman, D. G., Day, A. J., Willis, A. C., Sim, R. B., and Campbell, I. D. (1991) *Biochemistry* **30**, 997–1004
- Nagar, B., Jones, R. G., Diefenbach, R. J., Isenman, D. E., and Rini, J. M. (1998) *Science* **280**, 1277–1281
- Kirkitaadze, M. D., Jumel, K., Harding, S. E., Dryden, D. T. F., Krych, M., Atkinson, J. P., and Barlow, P. N. (1999) *Prog. Colloid Polymer Sci.* **113**, 164–167
- Kirkitaadze, M. D., Krych, M., Uhrin, D., Dryden, D. T. F., Smith, B. O., Cooper, A., Wang, X., Hauhart, R., Atkinson, J. P., and Barlow, P. N. (1999) *Biochemistry* **38**, 7019–7031
- Kirkitaadze, M. D., Dryden, D. T. F., Kelly, S. M., Price, N. C., Wang, X., Krych, M., Atkinson, J. P., and Barlow, P. N. (1999) *FEBS Lett.* **459**, 133–138
- Kraulis, P. J. (1991) *J. Appl. Crystallogr.* **24**, 946–950